

# PINHOLE CAMERA RESOLUTION AND EMITTANCE MEASUREMENT

C.A. Thomas\*, G. Rehm, Diamond Light Source, Oxfordshire, UK

## Abstract

Third generation synchrotron light sources are characterised by a low emittance and low emittance coupling. Some light sources are already proposing to operate with extremely low emittance coupling close to 0.1%. We derive the limits for the emittance coupling measurement due to the resolution of the X-ray pinhole camera. We also show that it is possible to design a pinhole camera in order to push the resolution limit beyond 0.1% emittance coupling. We then illustrate our calculations with the example of Diamond and compare them with experimental data.

## INTRODUCTION

Third generation synchrotron light sources are characterised by low emittance, and with the top-up operation becoming routine, they can afford to operate at extremely low emittance coupling. The measurement of the emittance can be done indirectly by measuring the transverse beam size. To this end, several devices, like Fresnel zone plates, interferometry, lens and camera or a pinhole camera, are currently used. All these systems have advantages but also limitations. Fresnel zone plates present the best possible resolution but they require monochromatic beam and the whole system can require significant effort to bring into routine operation [1, 2]. In addition, Fresnel zone plates cannot currently be produced for hard X-ray so these systems need to operate with soft X-rays, thus requiring all beam transport in vacuum. The lens and camera system is limited by the synchrotron radiation diffraction limits, which is of the order of 80  $\mu\text{m}$  in the visible. Such a system could be used with X-rays [3], but then the use of compound refractive lenses with X-rays requires also monochromatic light as they will introduce large chromatic aberrations, limiting the resolution of the system. Beam size measurement using interference methods also requires monochromatic light, and has a better resolution in the visible than visible light imaging system. However, due to the natural opening angle of the synchrotron radiation [4, 5], the maximum distance between the two slits is limited, hence defining the minimum measurable beam size.

At Diamond, we have chosen to use two X-ray pinhole cameras imaging the electron beam from two bending magnets, as they offer the required resolution and the dynamic range to accurately measure the electron beam size, typically  $50 \times 25 \mu\text{m}^2$  for 1% coupling, at all currents from below 1 mA to 500 mA [6]. Like any other optics system, it suffers from chromatic aberration, and a non optimised system may prevent measurement of an extremely small beam

size. However, optimisation of the X-ray pinhole system will give the possibility to measure very small beam sizes of typically less than 5  $\mu\text{m}$ .

## PSF OF THE X-RAY PINHOLE CAMERA

The performance of the measurement of the transverse electron beam size is given by the width of the point spread function (PSF) of the X-ray pinhole camera. The contributions to the PSF width are the PSF of the pinhole itself due to diffraction, and the PSF of the X-ray camera. The widths of these two contributions add quadratically to the total resolution of the X-ray pinhole camera, in the approximation of a Gaussian PSF.

### PSF of the Pinhole

We cannot experimentally measure the PSF from our pinholes, therefore, we calculate the PSF using the Fresnel integrals for the case of a square aperture. The calculation is performed in MATLAB, using the expression [7]:

$$I_\lambda(x, y, z) = I_{0\lambda}(x, y, z) \times \left| \int_{-a}^a e^{i2\pi \frac{(\xi - x_M)^2}{2\lambda\rho}} d\xi \int_{-b}^b e^{i2\pi \frac{(\eta - y_M)^2}{2\lambda\rho}} d\eta \right|^2 \quad (1)$$

with  $(x_M, y_M)$  the intersection point between the aperture plane and the straight  $P_0P$ ; the transverse plane is  $(x, y)$  and the propagation axis is  $(z)$ . The source is at  $P_0(x_0, y_0, z_0)$  and the image is at  $P(x, y, z)$ ;  $\lambda$  is the wavelength of the emitted light and  $\rho = -\frac{z z_0}{z - z_0}$  ( $z_0 < 0$ ). The aperture of the pinhole is  $2a$  and  $2b$  in each axis.

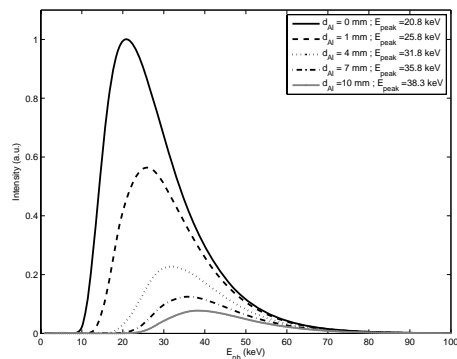


Figure 1: Spectrum of the Synchrotron radiation and filtered by Al window and 9 m of air. The thickness of the window and the peak of the spectrum are shown in the legend.

\* cyrille.thomas@diamond.ac.uk

For the calculation of the PSF of the pinhole, the spectrum of the source needs to be taken into account. In our case the spectrum is the synchrotron radiation from a bending magnet, filtered in energy and intensity by a 1 mm thick Al window, and several m of air. Figure 1 shows such a spectrum after 9 m of air and several thicknesses of Al. The result of the integration of expression 1 over the spectrum is the PSF of the pinhole at the screen. Examples of the PSF obtained for our second pinhole are given in figure 2. For large apertures, the PSF has a square shape close to the aperture size. While reducing the aperture width the width of the PSF goes through a minimum, which is the optimum working point for the pinhole. For monochromatic light this minimum is when the aperture is close to satisfying the relation  $2\lambda\rho = \pi a^2$ . When the aperture becomes smaller, the width of the PSF increases and the far field approximation is more valid.

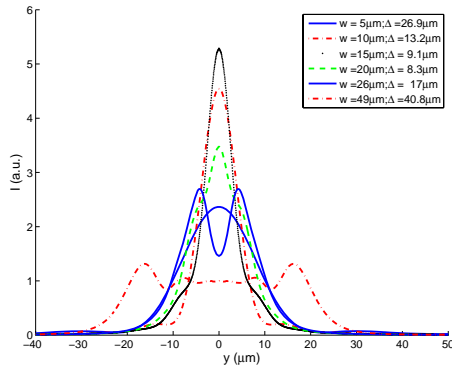


Figure 2: Normalised sum over the photon spectrum of the Fresnel diffraction patterns from a vertical slit of the bending magnet synchrotron radiation in Pinhole 2, and for several apertures.

In order to calculate the optimum working point for our pinholes, we evaluate the PSF for our two pinholes varying the aperture from 5  $\mu\text{m}$  to 50  $\mu\text{m}$ , and for several thicknesses of Al. Figure 3 shows the result for our second pinhole. For the 25  $\mu\text{m}$  aperture, the FWHM of the PSF are 16.8  $\mu\text{m}$  and 16.3  $\mu\text{m}$  for pinhole 1 and 2 respectively. However, the curves show that these are not the optimum working points. For apertures 18.3  $\mu\text{m}$  and 19.5  $\mu\text{m}$ , the PSF FWHM in pinhole 1 and 2 should be 7.5  $\mu\text{m}$  and 8.3  $\mu\text{m}$  respectively.

### PSF of the X-ray Camera

The X-ray camera is composed of an X-ray screen that converts absorbed X-ray photons into visible photons and a CCD camera that observes the screen through a macro-lens with a magnification close to 1. In order to directly measure the PSF of the system, we remove the pinhole and image the X-ray fan on the screen with an opaque mask with a sharp edge made by a tungsten bar covering part of the screen. We have been measuring the system resolution for several screen materials in different thicknesses:

06 Instrumentation, Controls, Feedback & Operational Aspects

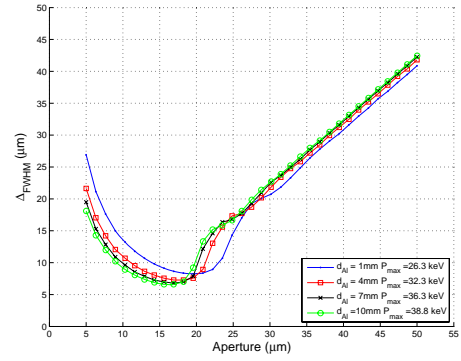


Figure 3: FWHM of the PSF from Pinhole 2 as function of the slit apertures and for several thickness of Al window.

Table 1: Width of the PSF (r.m.s) of the X-ray camera with several screens (in  $\mu\text{m}$ ). The error is given by the standard deviation of the fitted width per line on the digital image.

Thickness ( $\mu\text{m}$ )	P43	CdWO <sub>4</sub>	LuAG
5	6.2 $\pm$ 0.39	-	-
100	-	7.45 $\pm$ 0.45	-
200	-	8.45 $\pm$ 0.45	8.70 $\pm$ 0.45
400	-	-	10.0 $\pm$ 0.45
500	-	13.5 $\pm$ 0.45	-

P43 thickness 5  $\mu\text{m}$ , CdWO<sub>4</sub> thicknesses 500 and 200  $\mu\text{m}$ , and LuAG 400, 200 and 100  $\mu\text{m}$ . Table 1 summarises the results. The analysis performed is a fit using the error function of the response of the screen to the sharp edge. The result of the fit gives the r.m.s PSF of the screen. Figure 4 shows one such a measurement with P43 screen.

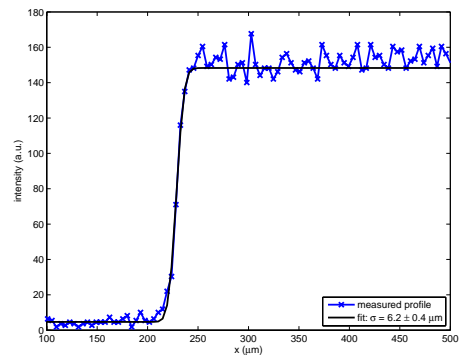


Figure 4: Resolution of the X-ray camera with P43 screen, measured using the sharp edge from a Tungsten bar in front of the screen. The r.m.s resolution is  $\Sigma_{screen} \approx 6 \mu\text{m}$ .

## EXPERIMENTAL RESULTS

The evaluation of the width of the PSF is essential for the measurement of the transverse beam sizes, but also to the calculation of emittance, energy spread, and precise emittance coupling.

T03 Beam Diagnostics and Instrumentation

Horizontal and vertical emittance are calculated using the following formula:

$$\sigma_i^2 = \beta_i \epsilon_i + (\eta_i \sigma_\epsilon)^2 \quad (2)$$

where  $\sigma_i$  is the measured beam size in the horizontal or vertical plane respectively ( $i = x, y$ ),  $\beta_i$  and  $\eta_i$  are the betatron and dispersion functions at the source point and in the corresponding plane; and  $\epsilon_i$  and  $\sigma_\epsilon$  are the emittance and the relative energy spread of the electron beam. The emittance coupling is often given as a percentage,  $K$ , of the horizontal emittance.

In the horizontal plane, we measure the emittance and the energy spread, being the solution of the two coupled equations with two unknown given by expression 2 for each of the two pinholes. The parameters  $\beta_x$  and  $\eta_x$  are assumed to be known. In practice, we measure the dispersion by varying the storage ring RF frequency by 100 Hz and retrieving the slope of the linear displacement of the centroid of the electron beam measured by the pinhole images. We also check the agreement with the data given by the linear optics measurements and optimisation procedure known as LOCO [8, 9]. In general, the agreement with the dispersion value is better than 1%. The betatron function at the source point is interpolated using the values given by LOCO.

In the vertical plane we assume the energy spread is known, so we have two equations and only one unknown, i.e. the emittance coupling. After applying the correction from LOCO, the dispersion measured is generally less than 1 mm. Although we could neglect the dispersion, for the measurement of small vertical emittance we still take it into account. If not, this would lead to over evaluate the vertical emittance. By applying corrections to the optics, we measured vertical beam sizes as small as 6  $\mu\text{m}$  on both pinholes, which corresponds to a vertical emittance of  $\epsilon_y \approx 2$  pm rad. Table 2 shows some of the results obtained with corrected optics. The good agreement between the two measurements is only due to the quadratic correction with the total PSF. Further agreement should be found with measurement of the betatron function at the source points.

## CONCLUSION

We have evaluated the PSF for the pinhole camera, taking into account the chromatic effects due to the large bandwidth of the source, which is synchrotron radiation from a bending magnet. This evaluation allows us to derive a more accurate resolution for the system as well as a set of parameters for an optimum working point. We also measured in situ the resolution of our X-ray camera. We can use the knowledge of the total resolution of the system for a deconvolution and measure thus extremely small vertical beam sizes, down to 6  $\mu\text{m}$ . Furthermore, the independent measurements of the vertical emittance using the two pinholes in our setup have shown a good correlation at a value as small as 2 pm rad.

Table 2: Vertical emittance measurements. Horizontal emittance and relative energy spread are measured close to the nominal values, i.e. 2.7 nm rad and 0.001 respectively. The betatron values are  $\beta_{y,1} = 21.54$  m and  $\beta_{y,2} = 23.38$  m. The magnification is  $m_{1,2} = 2.4, 2.7$  for Pinhole 1 and 2 respectively.  $\eta_i$  and  $\Sigma_i$  are measured values, and P stands for pinhole.

date		$\eta_y$ (mm)	$\Sigma_y$ ( $\mu\text{m}$ )	$\sigma_y$ ( $\mu\text{m}$ )	$\epsilon_y$ (pm rad)
				$= \frac{\sqrt{\Sigma_y^2 - \Sigma_0^2}}{m_i}$	$= \frac{\sigma_y^2 - \eta_y^2 \sigma_\epsilon^2}{\beta_y}$
CdWO <sub>4</sub> screen: Pinhole 1,2 $\Sigma_0 = 15.3, 15.1$ ( $\mu\text{m}$ )					
10/07	P 1	0.1	28	9.7	4.6
	P 2	0.1	32	10.6	4.9
12/07	P 1	0.7	21.5	6.3	1.8
	P 2	0.25	23.4	6.7	1.6
P43 screen Pinhole 1,2 $\Sigma_0 = 9.6, 9.4$ ( $\mu\text{m}$ )					
01/08	P 1	3	21	7.7	2.37
	P 2	5	25	8.6	2.08
02/08	P 1	0.1	19	6.8	2.18
	P 2	0.9	21	6.9	2.10

## REFERENCES

- [1] H. Sakai, M. Fujisawa, K. Iida, I. Ito, H. Kudo, N. Nakamura, K. Shinoe, T. Tanaka, H. Hayano, M. Kuriki, and T. Muto. Improvement of Fresnel zone plate beam-profile monitor and application to ultralow emittance beam profile measurements. *Physical Review Special Topics Accelerators and Beams*, 10(4):042801–18, April 2007.
- [2] C. David, V. Schlott, and A. Jaggi. A Zone Plate Based Beam Monitor for the Swiss Light Source. *Proceedings of DIPAC 2001*, pages 133–135, June 2001.
- [3] A. Snigirev, V. Kohn, I. Snigireva, and B. Lengeler. A compound refractive lens for focusing high-energy X-rays. *Nature*, 384:49–51, November 1996.
- [4] T. Mitsuhashi. Spatial Coherency of the Synchrotron Radiation at the Visible Light Region and its Application for Vertical Beam Profile Measurement. *APS Meeting Abstracts*, pages 3–, May 1997.
- [5] M. Arinaga, J. Flanagan, S. Hiramatsu, T. Ieiri, H. Ikeda, H. Ishii, E. Kikutani, T. Mimashi, T. Mitsuhashi, H. Mizuno, K. Mori, M. Tejima, and M. Tobiyama. KEB beam instrumentation systems. *Nuclear Instruments and Methods in Physics Research A*, 499:100–137, February 2003.
- [6] Thomas, C. A. and Rehm, G. DIAMOND Storage Ring Optical and X-ray Diagnostics. *Proceedings of BIW 2004*, Knoxville, Tennessee, 2004.
- [7] E. Hecht. *Optics*. Pearson Education, 4th edition, March 2004.
- [8] J. Safranek. Experimental determination of storage ring optics using orbit response measurements. *Nuclear Instruments and Methods in Physics Research A*, 388:27, 1997.
- [9] J. Safranek, G. Portmann, A. Terebilo, and C. Steier. MATLAB-BASED LOCO. In *Proceedings of EPAC*, pages 404–406, 2002.